Fig. 2. Two-sensor example.

It is clear from (2), that the path Γ specified by (3), is a function only of the ratio α_1/α_2. In Fig. 2 we plot the paths corresponding to three values of this ratio. The paths are plotted in Cartesian coordinates according to

$$\begin{pmatrix} x \\ y \end{pmatrix} = \begin{pmatrix} r\cos\theta \\ r\sin\theta \end{pmatrix}. \tag{4}$$

The upperbound on the probability of detection for a given false alarm rate can now be derived by computing (1) over the path Γ specified by (3).

CONCLUSIONS

We have introduced the concept of an upper bound to sensor fusion by way of determining the trajectory of a threat vehicle so that it affords the least overall total energy for detection into the sensor suite. Such a concept is useful in strategic route planning and for assessing tradeoffs between various possible sensor upgrades, that is, it can be used to guide expenditures so that the funds applied are applied in a well-balanced manner.

JOHN E. HERSHEY
AMER A. HASSAN
GUY R. SOHIE
General Electric Corporate Research
    and Development Center
1 River Road
Schenectady, NY 12301

REFERENCES

[1] Garvey, T. D., and Fischler, M. A. (1980)
        The integration of multi-sensor data for threat assessment.
        In *Proceedings of the 1980 Conference on Pattern
        Recognition*, 1980, 343–347.
[2] Hildebrand, F. B. (1952)
        Methods of Applied Mathematics.
        Englewood Cliffs, NJ: Prentice-Hall, 1952.
[3] Kazakos, D. (1988)
        Error bounds and asymptotic performance under mismatch
        of multisensor detection systems.
        Presented at the MIT-C3 Workshop, Monterey, CA, 1988.
[4] Van Trees, H. L. (1968)
        Detection, Estimation, and Modulation Theory, Part I.
        New York: Wiley, 1968.

[5] Wilber, G. F. (1988)
        Strategic route planning using informed best-first search.
        In *Proceedings of the IEEE 1988 National Aerospace
        and Electronics Conference* (NAECON'88), Vol. 3, 1988,
        1137–1144.

Spread-Spectrum Code and Carrier Synchronization Errors Caused by Multipath and Interference

The influence of multipath propagation and spread-spectrum interference on code and carrier synchronization is investigated. Both coherent and noncoherent delay lock loops (DLLs) are considered, with arbitrary early-late spacings up to one chip time. The coherent DLL is shown to have a major advantage; for a relatively high fading bandwidth, it has negligible tracking errors, while a noncoherent DLL always has a certain bias error. The results are particularly interesting for spread-spectrum positioning systems like Global Positioning System (GPS) and GLONASS.

I. INTRODUCTION

The effects of multipath propagation on spread-spectrum code and carrier tracking have already been investigated in a number of papers [1–8]. The majority of these focus on measurements or on a specific receiver architecture, which makes it difficult or even impossible to extrapolate the results to other environments or different types of receivers. The first analysis of multipath errors was given in [1]. This paper studied the effects of a single reflection on code tracking errors for the case of slow fading and a

one-chip early-late spacing. In [3, 4], it was discovered that receiver or antenna movements reduced the variance of Global Positioning System (GPS) code multipath errors. As explained in the next section, this is an effect of the increased fading bandwidth, which is an important parameter in the analysis of multipath tracking errors. Other investigations showed the beneficial effects of smaller early-late spacings on code multipath errors [6–8]. However, some questions still remain, especially about the effects of filtering of the spread-spectrum input signals and the role of the fading bandwidth, since all previous analyses (implicitly) assumed slow fading. The aim of this work is to discuss the remaining issues and to provide a simple way to predict the magnitude of code and carrier tracking errors in various environments, based on some knowledge of the multipath characteristics and the structure of the receiver used.

II. CODE AND CARRIER TRACKING ERRORS

If the presence of a certain number, say M, of multipath signals is taken into account, the received GPS signal from one satellite can be written as

$$x(t) = \sum_{i=0}^{M} a_i(t)p[t - \tau_i(t)]\cos[\omega t + \theta_i(t)] \qquad (1)$$

where $p(t)$ is the spread-spectrum code and $a_i(t)$, $\tau_i(t)$ and $\theta_i(t)$ denote the time-dependent amplitude, delay and phase of the ith signal, respectively. Noise is left out in (2), since the primary interest is the influence of multipath. The data signal $d(t)$ is also dropped, since its influence is removed by envelope detection in a noncoherent delay lock loop (DLL), or by decision-feedback in a coherent DLL. For simplicity of notation, the time dependence of the measured parameters a_i, τ_i, and θ_i is left out in the remainder of this work.

Note that in general all paths can have different frequencies $[\omega + \delta\theta_i(t)/\delta t]/2\pi$, where ω is the angular frequency of the line-of-sight signal. The bandwidth spread of these frequencies is called the *fading bandwidth*, which is a crucial parameter in the analysis of multipath tracking errors. For stationary receiver-reflector geometries (for instance reflections from the wings of an aircraft), the fading bandwidth is determined by the change of the satellite geometry only, which results in values that are usually much smaller than 1 Hz [2].

In order to track the line-of-sight signal delay, the input signal (1) is downconverted and correlated with an "early" and a "late" code. These are replicas of the received spread-spectrum code with a delay of plus and minus $d/2$ s compared with a "prompt" code, respectively. The parameter d is often referred to as the early-late spacing. If the loop is in lock, the delay of the prompt code is the desired delay estimate of

the input signal. In the case of a coherent DLL, the early and late correlation functions are subtracted to produce the "S-curve" $S_c(\tau)$:

$$S_c(\hat{\tau}_0) = \int_{t-T_{c0}}^{t} \sum_{i=0}^{M} a_i \cos[\theta_i - \hat{\theta}_0]$$
$$\cdot [R(\hat{\tau}_0 - \tau_i + d/2) - R(\hat{\tau}_0 - \tau_i - d/2)]\, dt$$

(2)

where $R(\tau)$ is the correlation function of the spread-spectrum code $p(t)$, correlated over a period of T_p seconds. d is the early-late spacing and $\hat{\theta}_0$ and $\hat{\tau}_0$ are the estimates of the receiver of the line-of-sight carrier phase θ_0 and delay τ_0, respectively. The correlation functions are averaged over a certain time T_{c0} that is usually much larger than T_p. The one-sided noise bandwidth $1/2T_{c0}$ of the averaging operation in (2) is referred to as the tracking loop bandwidth B_L.

In a noncoherent DLL, the S curve is formed by subtracting the squared early and late curves, thereby avoiding the need for carrier phase estimates.

$$S_{nc}(\hat{\tau}_0) = \int_{t-T_{c0}}^{t} \left| \sum_{i=0}^{M} a_i R(\hat{\tau}_0 - \tau_i + d/2)e^{j\theta_i} \right|^2$$
$$- \left| \sum_{i=0}^{M} a_i R(\hat{\tau}_0 - \tau_i - d/2)e^{j\theta_i} \right|^2 dt. \qquad (3)$$

Just like the coherent DLL, the noncoherent DLL tracks that value of $\hat{\tau}_0$ for which $S(\hat{\tau}_0)$ is zero while its slope $\delta S(\hat{\tau}_0)/\delta\hat{\tau}_0$ is negative.

The carrier tracking loop tracks the phase of the summed line-of-sight and multipath signals after correlation with the prompt code. Thus regardless of the type of code tracking loop, the carrier phase estimate can be expressed as

$$\hat{\theta}_0 = \arg\left(\int_{t-T_{ca}}^{t} \sum_{i=0}^{M} a_i e^{j\theta_i} R(\hat{\tau}_0 - \tau_i)\, dt \right). \qquad (4)$$

A. Slow Fading

To understand the effects of multipath propagation on code tracking, it is important to distinguish two different cases; the fading bandwidth B_F is large or small compared with the tracking loop bandwidth B_L. If B_F is small compared to B_L, then the averaging over T_{c0} or T_{ca} seconds in (2)–(4) has no influence on the resulting multipath tracking errors. In the case of one multipath signal ($M = 1$), maximum absolute delay errors occur if the multipath signal has a phase difference of 0 or 180 deg with the line-of-sight signal. This is because the phase of the sum signal is then equal to θ_0, assuming that the signal-to-multipath ratio (SMR) is greater than 1, so the multipath component in (2) gives a maximal distortion of the multipath free
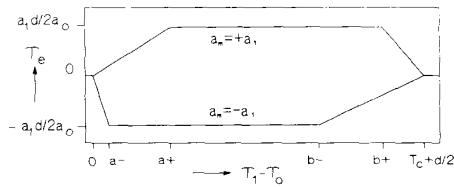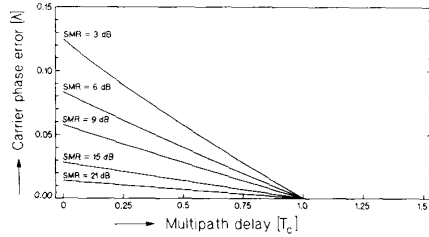
Fig. 1. Maximum and minimum delay errors.

Fig. 2. Amplitude of carrier tracking errors.

Fig. 3. Code and carrier range errors.

S curve. As proven in [7], maximum and minimum errors are equal to both coherent and noncoherent DLLs. Fig. 1 shows these errors as a function of the relative multipath delay $\tau_1 - \tau_0$. The figure is normalized with respect to the early-late spacing d and the SMR $= a_0^2/a_1^2$. In Fig. 1, $a\pm = (a_0 \pm a_1)d/2a_0$ and $b\pm = T_c - d[1 - (a_0 \pm a_1)/2a_0]$.

If the assumption is made that the influence of code tracking errors on the carrier phase errors is negligible, then it is also possible to give an analytical expression for the maximum carrier phase errors. This assumption is valid for small early-late spacings or for small SMR values. In this case, maximum and minimum carrier phase errors occur when the multipath vector is perpendicular to the sum vector. This results in an absolute phase error θ_e given by (5) and shown in Fig. 2:

$$\theta_e = \frac{1}{2\pi}\arcsin\left(\frac{\sqrt{1 - (\tau_1 - \tau_0)/T_c}}{\text{SMR}}\right) [\lambda]. \qquad (5)$$

Note that the phase error is given in wavelengths λ. To get the resulting GPS L1 and L2 carrier range errors, one has to multiply the results by 0.19 and 0.24 m, respectively. It is clear that multipath signals with small relative delays cause the largest phase errors because these signals are scarcely attenuated by the correlation operation. Equation (5) is valid for the case of specular reflections. In practical situations, diffuse reflections often occur, which can be described by a Rayleigh fading amplitude. However, as shown in [9], the resulting standard deviation in that case can be closely approximated as $\sqrt{2}/2$ times the error amplitude of (5).

Fig. 3 shows an example of GPS C/A-code and carrier range errors due to a reflection from a building. It clearly demonstrates the previously
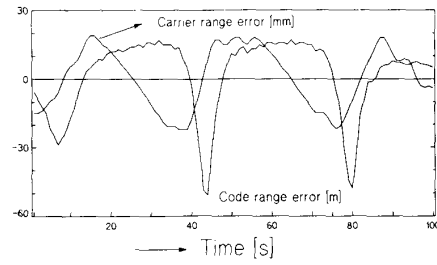
explained phenomenon that the absolute code tracking error is maximum when the carrier tracking error is zero, and reverse.

B. Fast Fading

If B_F is large compared with B_L, then most of the multipath components in (2) fall outside the passband of the equivalent DLL low-pass filter. This means that for a coherent DLL, only the line-of-sight component remains after averaging, which means that the tracking errors reduce to zero. Similarly, carrier tracking errors become negligible if B_F is large compared with B_{Lcar}. This is not the case for the noncoherent DLL, however. Because of the squaring operations in (3), one ends up with a time average in the case of fast fading that is equal to

$$S_{nc}(\hat{\tau}_0) = \sum_{i=0}^{M}[a_i R(\hat{\tau}_0 - \tau_i + d/2)]^2$$
$$- [a_i R(\hat{\tau}_0 - \tau_i - d/2)]^2. \qquad (6)$$

All cross products are filtered out because of their relatively high frequencies, so the resulting S-curve is simply the summation of $M + 1$ different noncoherent DLL S curves. This results in a certain tracking bias that is always positive. Examples of this bias in the case of $M = 1$ are depicted in Figs. 4(a) and (b) for an early-late spacing of one chip and one-tenth of a chip, respectively.

III. EFFECTS OF FILTERING

The previous analysis of multipath tracking errors assumed an infinite bandwidth of the spread-spectrum input signals. In practice, one always deals with filtered signals, causing the sharp edges of the S-curve to round. Now, there are three effects on multipath errors distinguishable. First, if the multipath amplitude is relatively small, that is within the approximately linear part of the line-of-sight S-curve, then due to the rounding of the multipath S-curve, the edges of Fig. 1 are also rounded. Second, due to the filtering, the slope of the S-curve at the desired zero crossing becomes smaller, thereby increasing the
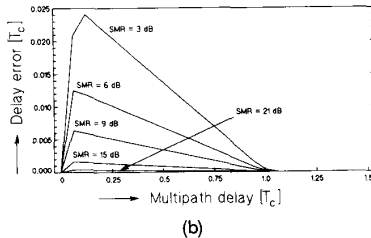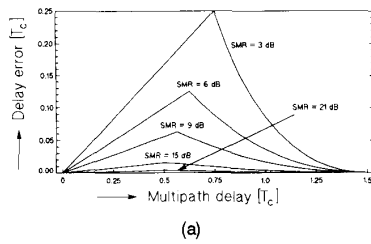
Fig. 4. (a) Bias of noncoherent DLL with $d = T_c$.
(b) Bias of noncoherent DLL with $d = T_c/10$.

Fig. 5. Multipath reduction factor versus early-late spacing.

multipath errors. To calculate the deterioration, precise knowledge of the filtered autocorrelation function $R(\tau)$ is required. For a single multipath signal, the maximum tracking error is equal to the amplitude of the filtered multipath S curve divided by the slope of the filtered line-of-sight S curve.

$$\tau_e = \lim_{\Delta \to 0} \frac{a_1 \left[R\left(\frac{T_c - d}{2}\right) - R\left(\frac{T_c + d}{2}\right) \right]}{2a_0 \left[R\left(\frac{d - \Delta}{2}\right) - R\left(\frac{d + \Delta}{2}\right) \right] / \Delta}.$$

(7)

If the signals are unfiltered, then $R(\tau) = 1 - |\tau/T_c|$ for $|\tau| < T_c$, and the formula for the maximum tracking error reduces to the well-known $da_1/2a_0$ from Fig. 1. In reality, however, the signals are always filtered. For the steep filters that are normally used in spread-spectrum receivers, the impulse response can be modeled quite accurately as $\text{sinc}[2\pi kt/T_c] \cdot k/T_c$, which is the response of an ideal rectangular low-pass filter with a double-sided bandwidth $BW = 2k/T_c$. This impulse response was used to calculate the filtered correlation function by performing a numerical convolution. Fig. 5 shows the tracking error τ_e divided by $T_c a_1/2a_0$ versus the early-late spacing d. For unfiltered signals, the resulting function is the dotted line. This means that for a specific value of d, the maximum code tracking errors are d/T_c smaller than in the case of a one chip early-late spacing. If the signals are filtered, it can be seen that this linear relation between d and the multipath errors no longer holds for small values of d; the error reduction factor converges to a value of about $1/T_c BW$, so there is no use in using an early-late spacing smaller than about $1/BW$.
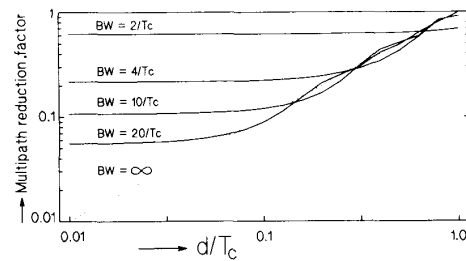
The third effect is that for relatively large multipath amplitudes that are outside the linear region of the line-of-sight S curve, the tracking errors become larger than predicted by (7). In the case of $a_1 = a_0$ (SMR = 1), the multipath errors even reach maximum and minimum values of plus and minus half a chip time, which is just as large as in the case of an early-late spacing of one chip time. For high SMR values, roughly above 10 dB, these nonlinear effects are very small so the previous analysis can be applied.

IV. SPREAD-SPECTRUM INTERFERENCE

In code division multiple access systems, specific spread-spectrum codes are used to distinguish between different transmitters. However, the codes that are used do not provide full orthogonality in general; different transmitters may interfere. Although the effects of spread-spectrum interference on the bit error probability are well known [10], to the best of the author's knowledge no one has studied the effects on the tracking performance. The next paragraph shows that spread-spectrum interference can simply be modeled in the same way as multipath.

Suppose two transmitters can be received, so the input signal is

$$x(t) = a_0 d_0(t - \tau_0) p_0(t - \tau_0) \cos(\omega_0 t + \theta_0)$$
$$+ a_1 d_1(t - \tau_1) p_1(t - \tau_1) \cos(\omega_1 t + \theta_1) \quad (8)$$

neglecting noise and multipath. The data signal of the ith transmitter is $d_i(t)$. To track the first signal, the input signal $x(t)$ is downconverted and correlated with $p_0(t - \hat{\tau}_0)$. However, besides the desired autocorrelation, at the same time a cross correlation with code $p_1(t - \tau_1)$ is obtained. Both auto and cross correlation functions consist of triangular pieces, so looking at the sum of auto and cross correlation functions, one cannot distinguish between cross correlation and multipath; both appear in the same form. However, there are two important differences. First, there are two different data signals present. If these two signals are uncorrelated, then their effect is that after the correlation operation, the interfering cross correlation component is spread

over the data bandwidth. In fact, the data bandwidth has the same effect as the fading bandwidth, so the previous multipath analysis also holds for the case of spread-spectrum interference.

When the delay of two GPS satellites is less than one bit time ($= 20$ ms), however, then the two data signals are certainly not uncorrelated, because of equal preambles and almanacs in the data. In this case, the influence of the data is largely removed, or even completely eliminated if the correlation is equal to one. If the data signals are correlated, or if the data bandwidth is smaller than the carrier frequency difference between the transmitters modulo, the code repetition frequency, then the latter parameter should be substituted as the fading bandwidth. For the SMR, the signal-to-interference ratio (SIR) $= a_0^2 / k a_1^2$ can be substituted, where k is the attenuation factor due to the correlation; for the GPS C/A-code, k is about 0.06. For the GPS P-code, interference can be neglected because of the enormous length of the code; if the input signal is correlated for 1 s, then the P-code interference is averaged over about 10^7 chips, while the C/A-code interference is effectively averaged over 1023 chips only, because of the C/A-code length of 1023 chips. As a result, the SIR is roughly 40 dB greater for the P-code, causing negligible errors.

A second characteristic of spread-spectrum interference is that cross correlation peaks can preceed the autocorrelation peak, as if they were multipath signals with a negative delay. This effect is also observed for long delayed multipath signals. Until now, multipath was modeled as a replica of the autocorrelation peak with a certain positive delay. If the delay exceeded $T_c + d/2$, the resulting multipath errors were zero. Unfortunately, the reality is more complicated; the autocorrelation function of the C/A-code contains similar unwanted peaks as the cross correlation function with an interfering code. Thus for delays exceeding $T_c + d/2$, there is always a possibility that an unwanted peak distorts the main peak. This unwanted peak again can be modeled as a multipath signal with a certain positive or negative delay that is equal to the delay of the main peak minus the delay of the interfering peak. It is easy to see that a multipath signal with positive delay τ_1 gives the same error, but with opposite sign, as a multipath signal with delay $-\tau_1$; independent of the type of loop or fading, $S(\tau_e \mid \tau_1) = -S(-\tau_e \mid -\tau_1)$. In words, the S curves for $+\tau_1$ and $-\tau_1$ are mirrored versions of each other. Thus if $+\tau_1$ gives a zero crossing at $\tau_e = \tau_{e1}$, then $-\tau_1$ gives a zero crossing at $\tau_e = -\tau_{e1}$. The conclusion is that all previously shown figures on multipath errors as a function of the multipath signal delay also apply to negative delays by simply multiplying everything by -1.

An interesting fact in the case of two interfering transmitters is that the resulting errors have the same form, but are exactly out of phase. If the input signal (8) is correlated with $p_0(t - \hat{\tau}_0)$ and $p_1(t - \hat{\tau}_1)$ for T s,

the following output signals are obtained, neglecting the carrier phases:

$$\int_0^T [a_0 p_0(t - \tau_0) + a_1 p_1(t - \tau_1)] p_0(t - \hat{\tau}_0) \, dt$$
$$= a_0 R_0(\hat{\tau}_0 - \tau_0) + a_1 R_c(\hat{\tau}_0 - \tau_1)$$
$$\int_0^T [a_0 p_0(t - \tau_0) + a_1 p_1(t - \tau_1)] p_1(t - \hat{\tau}_1) \, dt \tag{9}$$
$$= a_1 R_1(\hat{\tau}_1 - \tau_1) + a_0 R_c(\hat{\tau}_1 - \tau_0).$$

Here, $R_c(\tau)$ is the cross correlation function of $p_0(t)$ and $p_1(t)$. From (9), it can be seen that the cross correlation function has a delay of $\tau_1 - \tau_0$ compared with the autocorrelation function for the first term of (9), while the delay is $\tau_0 - \tau_1$ for the second term. Thus if the correlation function of the first transmitter is distorted by a cross-correlation peak with a positive delay, the second one suffers from exactly the same peak, but now with a negative delay. Also, the SIR values of $a_0^2 / k a_1^2$ and $a_1^2 / k a_0^2$ are different in general, because of differences in received signal powers. For instance, if a certain GPS satellite is received 20 dB stronger than another one, the latter will suffer from a SIR of 3 dB, resulting in C/A-code tracking errors of tens of meters in the case of slow fading.

An example of GPS satellite interference is depicted in Figs. 6(a) and (b), which show C/A-code range errors from a receiver with a noncoherent DLL. Both satellites have approximately the same error curve, but with opposite sign, as predicted in the previous analysis. The correlation value between the errors of 6(a) and 6(b) is -0.8, see Fig. 6(d). From Fig. 6(c), one can see that the Doppler difference between the two satellites changes sign at the middle of the measurement. As a result, the second half of Figs. 6(a) and 6(b) is a mirrored version of the first part. Since the Doppler difference is much larger than the loop bandwidth most of the time, the fading is fast, so Figs. 6(a) and 6(b) depict the bias errors of a noncoherent DLL, while the interference delay is gradually changing because of the Doppler difference. Similar measurements with a coherent DLL did not show any significant effects due to interference, which confirms the theory that a coherent DLL simply rejects interfering signals with frequency differences exceeding the tracking loop bandwidth.

V. PREDICTED ERROR VALUES

If expected values of SMR, B_F, and multipath delay τ is a specific environment are known, then it is possible to predict the multipath error level from the presented model. Typical multipath parameters for circulary polarized L-band signals (like GPS) in different environments can be found in [11–13]. Table I summarizes the SMR, B_F and τ values of these references, together with a prediction of the mean
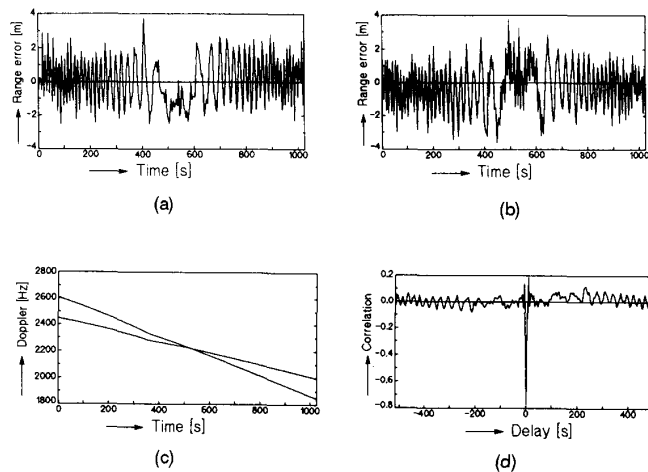
Fig. 6. (a) Interference errors of sv11 due to sv21. (b) Interference errors of sv11 due to sv21. (c) Doppler frequencies of sv11 and sv21. (d) Cross correlation of 11(a) and 11(b).

TABLE I
Typical Multipath Parameter Values for Different Environments

Environment	SMR [dB]	B_F [Hz]	$\tau[\mu s]$	C/A-code errors [m] σ	Carrier errors [cm] μ	σ
Maritime	10	4	0.05	4	1.5	0.8
Aeronautical, ground reflections	15	30	0–30	3	5	0.4
Aeronautical, wing reflections	20	0.02	0.02	2	< 0.01	0.2
Land mobile, rural/suburban						
$v = 10$ m/s	5	100	0.3	4	18	1.0
$v = 0$ m/s	5	0.1	0.3	33	1.5	1.3

(μ) and standard deviation (σ) of the resulting GPS C/A-code and carrier errors. For SMR values larger than about 10 dB, the standard deviation of code range errors can be approximated as $\sqrt{2}/2$ times half the top-top error shown in Fig. 1, where a_0/a_1 should be substituted by $\sqrt{SMR}$. Precise values of σ and μ can be found in [9]. The presented values are only rough estimates, because they strongly depend on the specific environment, antenna, elevation angle, height and speed of the receiver. Nevertheless, the estimated range errors give an indication of what can be expected in various situations.

The GPS range errors are predicted for the case of a noncoherent DLL with a loop bandwidth of 1 Hz, an early-late spacing of one chip and a carrier tracking loop bandwidth of 20 Hz. To calculate the standard deviation of the errors in the case of fast fading $(B_F > B_L)$, it is assumed that the effective SMR is approximately reduced by a factor B_L/B_F, assuming the Doppler spectrum is flat over a bandwidth B_F. In

the case of a coherent DLL, the mean errors become considerably smaller, except for the cases of very small fading bandwidths. Further reductions can be achieved by using a DLL with a smaller loop bandwidth, which is possible if carrier-rate aided tracking is applied. Because of receiver dynamics, it is not possible to considerably lower the carrier tracking loop bandwidth; therefore, the given phase error estimates apply to almost all available GPS receivers.

If the early-late spacing is reduced to one-tenth of a chip, then the σ values are reduced by almost a factor ten in the land mobile and aeronautical ground reflection cases, while the other values stay approximately the same, because their multipath delay is less than the early-late spacing. An interesting fact is that P-code errors are approximately the same as C/A-code errors with $d = T_c/10$, except in cases where the multipath delay exceeds the P-code chip time $T_{cp} = 100$ ns. Since the P-code is transmitted with a bandwidth of approximately $2/T_{cp}$, the beneficial effects of using an early-late spacing smaller than one chip are very small, as indicated in Fig. 5.

VI. CONCLUSIONS

In the analysis of multipath errors, the ratio of fading bandwidth and loop bandwidth turned out to be a crucial parameter; for small B_F/B_L values, one suffers from slowly time-varying errors. The envelope of these errors is exactly equal for coherent and noncoherent DLLs, regardless of the early-late spacing. For large B_F/B_L values, a coherent DLL has negligible errors, while a noncoherent DLL ends up with a certain bias. Thus for situations where fast fading can be expected, a coherent DLL is preferable in order to minimize multipath and interference errors in the code ranges.

Maximum absolute multipath code range errors are proportional to the early-late spacing d, reaching a maximum of $d/2$ if the SMR reaches 1. However, filtering of the spread-spectrum signals causes an increase of the multipath errors. If the SMR approaches 1, the errors can still reach maximum and minimum values of $\pm T_c/2$ (± 150 m for the GPS C/A-code), independent of the early-late spacing.

Spread-spectrum interference can be analyzed in the same way as multipath. GPS ranging errors of several meters were measured, but the analysis showed that much stronger errors can occur when there are large power differences between received signals. Because of its insensitivity to fast fading, a coherent DLL is affected much less by interference than a noncoherent DLL.

As a final remark, it should be noted that multipath errors are not unavoidable; conventional tracking loops are simply not designed to deal with multipath or spread-spectrum interference. By changing the receiver structure, considerable improvements can be achieved [14]. By using a receiver as described in [14], the performance becomes limited by noise only, rather than by multipath or interference.

ACKNOWLEDGMENT

The author wishes to thank P. Kranendonk and X. Jin for their help with the GPS measurements.

RICHARD D. J. VAN NEE
Telecommunications and Traffic Control Systems Group
Delft University of Technology
P.O. Box 5031
2600 GA Delft
The Netherlands

REFERENCES

[1] Hagerman, L. L. (1973)
     Effects of multipath on coherent and noncoherent PRN ranging receiver.
     Report TOR-0073(3020-03)-3, Development Planning Division, The Aerospace Corporation, May 15, 1973.

[2] van Nee, D. J. R. (1991)
     Multipath effects on GPS code phase measurements.
     In Proceedings of Institute of Navigation, GPS-91, Albuquerque, NM, Sept. 1991, 915–924.

[3] Braasch, M. S., and Van Graas, F. (1991)
     Guidance accuracy issues for realtime GPS interferometric attitude and heading determination.
     In Proceedings of the Institute of Navigation, GPS-91, Albuquerque, NM, Sept. 1991, 373–386.

[4] Lachapelle, G., Falkenberg, W., Neufeldt, D., and Kielland, P. (1989)
     Marine DGPS using code and carrier in a multipath environment.
     In Proceedings of the Institute of Navigation, GPS-89, Colorado Springs, CO, Sept. 1989, 343–347.

[5] Tranquilla, J. M., and Carr, J. P. (1990)
     GPS multipath field observations at land and water sites.
     Navigation, Journal of the Institute of Navigation, 37, 4 (Winter 1990–1991), 393–414.

[6] van Dierendonck, A. J., Fenton, P., and Ford, F. (1992)
     Theory and performance of narrow correlator spacing in a GPS receiver.
     In Proceedings of the ION National Technical Meeting, San Diego, CA, Jan. 27, 1992.

[7] van Nee, D. J. R. (1992)
     Reducing multipath tracking errors in spread-spectrum ranging systems.
     Electronics Letters, 28, 8 (Apr. 1992), 729–731.

[8] Braasch, M. S. (1992)
     On the characterization of multipath errors in satellite-based precision approach and landing systems.
     Ph.D. dissertation, Ohio University, Athens, June, 1992.

[9] van Nee, D. J. R. (1993)
     The influence of GPS multipath errors on the position reference system.
     Contract report for the National Aerospace Laboratory of The Netherlands, contract Et 92.085, Feb. 9, 1993.

[10] Pursley, M. B. (1977)
     Performance evaluation for phase-coded spread-spectrum multiple-access communication-part I: System analysis.
     IEEE Transactions on Communications, 25, 8 (Aug. 1977), 795–799.

[11] Van Rees, J. (1987)
     Measurements of the wide-band radio channel characteristics for rural, residential, and suburban areas.
     IEEE Transactions on Vehicular Technology, VT-36, 1 (Feb. 1987), 2–6.

[12] Jongejans, A., et al. (1986)
     Prosat phase I report.
     European Space Agency, STR-216, European Space Research and Technology Organization, Noordwijk, The Netherlands, May 1986.

[13] Ohmori, S., et al. (1992)
     Experiments on aeronautical satellite communications using ETS-V satellite.
     IEEE Transactions on Aerospace and Electronic Systems, 28, 3 (July 1992), 788–795.

[14] van Nee, D. J. R. (1992)
     The multipath estimating delay lock loop.
     Presented at the IEEE 2nd International Symposium on Spread Spectrum Techniques and Applications, Yokohama, Japan, Nov. 29–Dec. 2, 1992.

Errata: The Hit Array: A Synthesis Tool For Multiple Access Frequency Hop Signals

Mr. Ivan Šeškan should have appeared as one of the authors of "The Hit Array: A Synthesis Tool for Multiple Access Frequency Hop Signals," this journal, **29**, 3 (July 1993), 624–635.